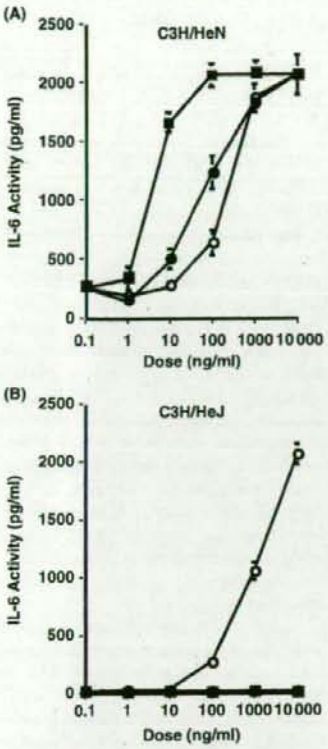

Fig. 8. Induction of IL-6 release from murine peritoneal macrophages from C3H/HeN and C3H/HeJ mice stimulated by *Porphyromonas gingivalis* synthetic lipid A. Stimulation of peritoneal macrophages was performed as well as that of TNF-α, and IL-6 activity in the supernatants was determined by an ELISA kit. The results are expressed as means ± SD of duplicate experiments. ●, synthetic Pg-LA; ○, native lipid A; ■, compound 506.

LPS-unresponsive mice appears to be induced by bioactive contaminants such as LPS protein (54) and other microbial components present in the native preparations. Ogawa's group recently suggested that *P. gingivalis* purified natural lipid A and compound 381 lacked the ability to activate gingival fibroblasts from C3H/HeJ, TLR4 knockout and myeloid differentiation factor 88 knockout mice (35), and also a triacylated lipoprotein, consisting of two palmitoyl groups and one pentadecanoyl group at the N-terminal of glycerocysteine from *P. gingivalis* lipid A, is a principal component for TLR2-mediated cell activation (13, 28). On the other hand, Darveau's group seem to have considered the possibility that multiple lipid A species of *P. gingivalis* may functionally interact with both TLR2 and TLR4, such as the under acylated lipid A moiety activate cells through TLR2 (6, 7).

IL-8 induction activity of synthetic Pg-LA to HGFs was significantly inhibited by polymyxin B in this study. However, no inhibitory effects of polymyxin B were observed on the immune responses of native *P. gingivalis* lipid A. The results were similar to those of other reports that the effect of polymyxin B on *P. gingivalis* LPS was relatively low (23). Polymyxin B may neutralize the endotoxicity of active-type molecules present in *P. gingivalis* LPS by binding to phosphate groups in the lipid A part (31), but may not inhibit the immune responses induced by the other contaminating bacterial components that act through the TLR2 pathway. This may be one of the reasons for the low inhibitory potency of polymyxin B to *P. gingivalis* LPS, in addition to the factors affecting the LPS-neutralization potency such as the absence of a phosphate group at position 4′ and presence of a polar head group in the native lipid A (26).

Anti-human CD14 mAb inhibited both IL-8 production from HGFs and TNF-α production from human monocytoid MM6-CA8 cells by synthetic Pg-LA as described in this study. On the other hand, it has been reported that anti-murine CD14 mAb could block *P. gingivalis* LPS-mediated immune responses (50) that may be mediated through both TLR2 and TLR4. These findings suggested that CD14 associates closely with not only the TLR4 but also the TLR2 signaling pathway mediated by *P. gingivalis* LPS. This was also supported by our previous report (54) that the LPS-antagonist, succinylated lipid A precursor (succinylated 406), inhibited TNF-α induction activity of *P. gingivalis* native lipid A in peritoneal macrophages from C3H/HeN and C3H/HeJ mice. In addition B464, a low-toxicity lipid A analog (62), significantly inhibited TNF-α production from human monocytoid MM6-CA8 cells induced by *P. gingivalis* native and synthetic lipid A (data not shown). Succinylated 406 and B464 competitively inhibit LPS action at the same stages in the LPS signaling pathway involving LBP, CD14 and TLRs. Taking these points into consideration, both LPS inhibitors appear to suppress the immune responses through CD14 and the TLR family including TLR2, by blocking the function of CD14 in the signaling cascade.

In conclusion, these findings suggested that the moderated and reduced biological activity of *P. gingivalis* LPS and native lipid A, including the activity on C3H/HeJ mouse cells via the TLR2-mediated pathway, may be mediated by bioactive contaminants or low acylated molecules present in the native preparations having high heterogeneity in lipid A moiety. To elucidate these problems, we are now attempting to evaluate the biological characterizations of tetra-acylated monophosphorylated or diphosphorylated species with the predominant molecules found in *P. gingivalis* native lipid A, using each chemically synthesized analog.

Acknowledgments

We would like to thank Dr Shoichi Kusumoto for helpful advice in the synthesis process of lipid A. We would also like to thank Drs Toshimi Murai and Yukari Nakagawa for helpful advice on the culture method of MM6-CA8 cells and Daiichi Pharmaceutical Co. for providing *Escherichia coli*-type synthetic lipid A (compound 506). This work was supported in part by grants from the Ministry of Education,

Table 3. Effects of mAbs on the production of TNF-α by human monocytoid MM6-CA cells stimulated with *P. gingivalis* synthetic lipid A

	Stimulants *P. gingivalis* lipid A					
	Native		Synthetic		Compound 506	
mAbs	TNF-α release[1]	% control	TNF-α release[1]	% control	TNF-α release[1]	% control
Non	118.0 ± 2.1	100.0	428.6 ± 45.6	100.0	420.8 ± 48.9	100.0
Anti-TLR2	65.0 ± 3.0	55.1	398.2 ± 89.5	92.9	396.0 ± 22.2	94.1
Anti-TLR4	67.0 ± 0.2	56.8	5.7 ± 3.1	1.3	11.5 ± 3.6	2.7
Anti-TLR2 + TLR4	35.0 ± 3.6	29.7	18.2 ± 7.8	4.2	40.3 ± 5.6	9.6
Anti-CD14	38.0 ± 2.1	32.2	3.8 ± 1.2	0.9	3.4 ± 1.1	0.8

[1]TNF-α release in pg/ml. Dose of each antibody: anti-human TLR2 mAb TL2.1, 5 μg/ml; anti-human TLR4/MD-2 complex mAb HTA125, 5 μg/ml; anti-human CD14 mAb MY4, 10 μg/ml. Dose of each lipid: *Porphyromonas gingivalis* native lipid A, 10 ng/ml; *P. gingivalis* synthetic lipid A, 1 ng/ml; compound 506, 1 ng/ml.

Science and Culture (17592170 to H.K. and 04671111 to Y.H.)

References

1. Abreu MT, Fukata M, Arditi M. TLR signaling in the gut in health and disease. J Immunol 2005: **174**: 4453–4460.
2. Aliprantis AO, Yang RB, Mark MR et al. Cell activation and apoptosis by bacterial lipoproteins through toll-like receptor-2. Science 1999: **285**: 736–739.
3. Al-Qutub MN, Braham PH, Karimi-Naser LM, Liu X, Genco CA, Darveau RP. Hemin-dependent modulation of the lipid A structure of *Porphyromonas gingivalis* lipopolysaccharide. Infect Immun 2006: **74**: 4474–4485.
4. Anderson KV. Toll signaling pathways in the innate immune response. Curr Opin Immunol 2000: **12**: 13–19.
5. Burgess K, Jennings LD. Enantioselective esterifications of unsaturated alcohols mediated by a lipase prepared from *Pseudomonas* sp. J Am Chem Soc 1991: **113**: 6129–6139.
6. Darveau RP, Pham TT, Lemley K et al. *Porphyromonas gingivalis* lipopolysaccharide contains multiple lipid A species that functionally interact with both Toll-like receptors 2 and 4. Infect Immun 2004: **72**: 5041–5051.
7. Dixon DR, Darveau RP. Lipopolysaccharide heterogeneity: innate host responses to bacterial modification of lipid A structure. J Dent Res 2005: **84**: 584–595.
8. Fujiwara T, Ogawa T, Sobue S, Hamada S. Chemical, immunobiological and antigenic characterizations of lipopolysaccharides from *Bacteroides gingivalis* strains. J Gen Microbiol 1990: **136**: 319–326.
9. Fukase K, Kurosawa S, Kusumoto S. Synthesis and purification by HPLC of de-*O*-acyl partial structures of *Escherichia coli* Re lipopolysaccharide. J Endotoxin Res 1994: **1**: 149–163.
10. Galanos C, Lüderitz O, Westphal O. Preparation and properties of a standardized lipopolysaccharide from *Salmonella abortus equi*. Zentralbl Bakteriol (Orig A) 1979: **243**: 226–244.
11. Guo L, Lim KB, Gunn JS et al. Regulation of lipid A modifications by *Salmonella typhimurium* virulence genes phoP-phoQ. Science 1997: **276**: 250–253.
12. Hamada S, Takada H, Mihara J, Nakagawa I, Fujiwara T. LPS of oral *Bacteroides* species: general properties and induction of cytokines in human gingival fibroblast cultures. In: Nowotny A, Spitzer JJ, Ziegler EJ, ed. Cellular and molecular aspects of endotoxin reactions. Amsterdam: Elsevier Science Publishers, 1990: 285–294.
13. Hashimoto M, Asai Y, Ogawa T. Separation and structural analysis of lipoprotein in a lipopolysaccharide preparation from *Porphyromonas gingivalis*. Int Immunol 2004: **16**: 1431–1437.
14. Hirschfeld M, Ma Y, Weis JH, Vogel SN, Weis JJ. Repurification of LPS eliminates signaling through both human and murine Toll-like receptor 2. J Immunol 2000: **165**: 618–622.
15. Holt SC, Ebersole J, Felton J, Brunsvold M, Kornman S. Implantation of *Bacteroides gingivalis* in nonhuman primates initiates progression of periodontitis. Science 1988: **239**: 55–57.
16. Homma JY, Matsuura M, Kanegasaki S et al. Structural requirements of lipid A responsible for the functions: a study with chemically synthesized lipid A and its analogues. J Biochem 1985: **98**: 395–406.
17. Hoshino K, Takeuchi O, Kawai T et al. Toll-like receptor 4 (TLR4)-deficient mice are hyporesponsive to lipopolysaccharide: evidence for TLR4 as the Lps gene product. J Immunol 1999: **162**: 3749–3752.
18. Iiño Y, Hopes RM. The bone resorbing activities in tissue culture of lipopolysaccharides from the bacteria *Actinobacillus actinomycetemcomitans*, *Bacteroides gingivalis*, and *Capnocytophaga ochracea* isolated from human mouths. Arch Oral Biol 1984: **29**: 59–63.
19. Imoto M, Yoshimura H, Shimamoto T, Sakaguchi N, Kusumoto S, Shiba T. Total synthesis of *Escherichia coli* lipid A, the endotoxically active principle of cell-surface lipopolysaccharide. Bull Chem Soc Jpn 1987: **60**: 2205–2214.
20. Inage M, Chaki H, Imoto M, Shimamoto T, Kusumoto S, Shiba T. Synthetic approach to lipid As: preparation of phosphorylated disaccharides containing (*R*)-3-hydroxyacyl and (*R*)-3-acyloxyacyl groups. Tetrahedron Lett 1983: **24**: 2011.
21. Kato H, Haishima Y, Iida T, Tanaka A, Tanamoto K. Chemical structure of lipid A isolated from *Flavobacterium meningosepticum* lipopolysaccharide. J Bacteriol 1998: **180**: 3891–3899.
22. Kawahara K, Tsukano H, Watanabe H, Lindner B, Matsuura M. Modification of the structure and activity of lipid A in *Yersinia pestis* lipopolysaccharide by growth temperature. Infect Immun 2002: **70**: 4092–4098.
23. Kirikae T, Nitta T, Kirikae F et al. Lipopolysaccharides (LPS) of oral black-pigmented bacteria induce tumor necrosis factor production by LPS-refractory C3H/HeJ macrophages in a way different from that of *Salmonella* LPS. Infect Immun 1999: **67**: 1736–1742.
24. Koga T, Nishihara T, Fujiwara T et al. Biochemical and immunobiological properties of lipopolysaccharide (LPS) from *Bacteroides gingivalis* and comparison with LPS from *Escherichia coli*. Infect Immun 1985: **47**: 638–647.
25. Kumada H, Haishima Y, Kondo S, Umemoto T, Hisatsune K. Occurrence of 2-keto-3-deoxyoctonate (KDO) and KDO phosphate in lipopolysaccharides of *Bacteroides* species. Curr Microbiol 1993: **26**: 239–244.
26. Kumada H, Haishima Y, Umemoto T, Tanamoto K. Structural study on the free lipid A isolated from lipopolysaccharide of *Porphyromonas gingivalis*. J Bacteriol 1995: **177**: 2098–2106.
27. Kumada H, Watanabe K, Umemoto T, Kato K, Kondo S, Hisatsune K. Chemical and biological properties of lipopolysaccharide, lipid A and degraded polysaccharide from *Wolinella recta* ATCC 33238. J Gen Microbiol 1989: **135**: 1017–1025.
28. Makimura Y, Asai Y, Taiji Y, Sugiyama A, Tamai R, Ogawa T. Correlation between chemical structure and biological activities of *Porphyromonas gingivalis* synthetic lipopeptide derivatives. Clin Exp Immunol 2006: **146**: 159–168.
29. Mansheim BJ, Onderdonk AB, Kasper DL. Immunochemical and biological studies of the lipopolysaccharide of *Bacteroides melaninogenicus* subspecies *asaccharolyticus*. J Immunol 1978: **120**: 72–78.
30. Medzhitov R, Preston-Hurlburt P, Janewy CA Jr. A human homologue of the *Drosophila* Toll protein signals activation of adaptive immunity. Nature 1997: **388**: 394–397.
31. Morrison DC, Danner RL, Dinarello CA et al. Bacterial endotoxins and pathogenesis of Gram-negative infections: current status and future direction. J Endotoxin Res 1994: **1**: 71–83.
32. Nair BC, Mayberry WR, Dziak R, Chen PB, Levine MJ, Hausmann E. Biological effects of a purified lipopolysaccharide from *Bacteroides gingivalis*. J Periodontal Res 1983: **18**: 40–49.
33. Nashed MA, Anderson L. Iodine as a reagent for the ready hydrolysis of prop-1-enyl glycosides, or their conversion into oxazolines. J Chem Soc Chem Commun 1982: **21**: 1274–1276.
34. Obayashi T, Tamura H, Tanaka S et al. A new chromogenic endotoxin-specific assay using recombined limulus coagulation enzymes and its clinical applications. Clin Chim Acta 1985: **149**: 55–65.
35. Ogawa T, Asai Y, Hashimoto M et al. Cell activation by *Porphyromonas gingivalis* lipid A molecule through Toll-like receptor 4- and myeloid differentiation factor 88- dependent signaling pathway. Int Immunol 2002: **14**: 1325–1332.
36. Ogawa T, Asai Y, Yamamoto H et al. Immunobiological activities of a chemically synthesized lipid A of *Porphyromonas gingivalis*. FEMS Immunol Med Microbiol 2000: **28**: 273–281.
37. Ogawa T, Uchida H, Amino K. Immunobiological activities of chemically defined lipid A from lipopolysaccharides of *Porphyromonas gingivalis*. Microbiology 1994: **140**: 1209–1216.
38. Oltvoort JJ, Van Boeckel CAA, De Koning JH, Van Boom JH. Use of the cationic iridium complex 1,5-cyclooctadiene-bis[methyldiphenylphosphine]-iridium hexa fluorophosphate in carbohydrate chemistry: smooth isomerization of allyl ethers to 1-propenyl ethers. Synthesis 1981: **1981**: 305–308.
39. Poltorak A, He X, Smirnova I et al. Defective LPS signaling in C3H/HeJ and C57BL/10ScCr mice: mutations in *Tlr4* gene. Science 1998: **282**: 2085–2088.
40. Qureshi N, Takayama K. Purification and structural determination of nontoxic lipid A obtained from the lipopolysaccharide of *Salmonella typhimurium*. J Biol Chem 1982: **257**: 11808–11815.
41. Qureshi N, Takayama K, Meyer KC et al. Chemical reduction of 3-oxo and unsaturated

groups in fatty acids of diphosphoryl lipid A from the lipopolysaccharide of *Rhodopseudomonas sphaeroides*. J Biol Chem 1991: **266**: 6532–6538.

42. Rietschel ET, Brade L, Schade U et al. Bacterial endotoxins: properties and structure of biologically active domains. In: Schrinner E, Richmond MH, Seibert G, Schwarz U, ed. Surface structures of microorganisms and their interactions with the mammalian host. Weinheim, Germany: VCH Verlagsgesellschaft mbH, 1988: 1–41.
43. Rosenstreich DL, Glode LM. Differences in B cell mitogen responsiveness between closely related strains of mice. J Immunol 1975: **115**: 777–780.
44. Schifferle RE, Reddy MS, Zambon JJ, Genco RJ, Levine MJ. Characterization of a polysaccharide antigen from *Bacteroides gingivalis*. J Immunol 1989: **143**: 3035–3042.
45. Shimazu R, Akashi S, Ogata H et al. MD-2, a molecule that confers lipopolysaccharide responsiveness on Toll-like receptor 4. J Exp Med 1999: **189**: 1777–1782.
46. Skidmore BJ, Morrison DC, Chiller JM, Weigle WO. Immunologic properties of bacterial lipopolysaccharide (LPS). II. The unresponsiveness of C3H/HeJ mouse spleen cells to LPS-induced mitogenesis is dependent on the method used to extract LPS. J Exp Med 1975: **142**: 1488–1508.
47. Slots J, Genco RJ. Microbial pathogenicity. Black pigmented *Bacteroides* species, *Capnocytophaga* species, and *Actinobacillus actinomycetemcomitans* in human periodontal disease: virulence factors in colonization, survival, and tissue destruction. J Dent Res 1984: **63**: 412–421.
48. Soejima K, Ishizaka A, Urano T et al. Protective effect of B464, a lipid A analog, on endotoxin-induced cellular responses and acute lung injury. Am J Resp Crit Care Med 1996: **154**: 900–906.
49. Suda Y, Kirikae T, Shiyama T et al. Macrophage activation in response to S-form lipopolysaccharides (LPS) separated by centrifugal partition chromatography from wild-type LPS: effects of the *O*-polysaccharide portion of LPS. Biochem Biophys Res Commun 1995: **210**: 678–685.
50. Tabeta K, Yamazaki K, Akashi S et al. Toll-like receptors confer responsiveness to lipopolysaccharide from *Porphyromonas gingivalis* in human gingival fibroblasts. Infect Immun 2000: **68**: 3731–3735.
51. Takada H, Mihara J, Morisaki I, Hamada S. Induction of interleukin-1 and -6 in human gingival fibroblast cultures stimulated with *Bacteroides* lipopolysaccharides. Infect Immun 1991: **59**: 295–301.
52. Takeda K, Akira S. Toll-like receptors in innate immunity. Int Immunol 2005: **17**: 1–14.
53. Takeuchi O, Hoshino K, Kawai T et al. Differential roles of TLR2 and TLR4 in recognition of gram-negative and gram-positive bacterial cell wall components. Immunity 1999: **11**: 443–451.
54. Tanamoto K, Azumi S, Haishima Y, Kumada H, Umemoto T. The lipid A moiety of *Porphyromonas gingivalis* lipopolysaccharide specifically mediates the activation of C3H/HeJ mice. J Immunol 1997: **158**: 4430–4436.
55. Tanamoto K, Azumi S, Haishima Y, Kumada H, Umemoto T. Endotoxic properties of free lipid A from *Porphyromonas gingivalis*. Microbiology 1997: **143**: 63–71.
56. Tanamoto K, Kato H, Haishima Y, Azumi S. Biological properties of lipid A isolated from *Flavobacterium meningosepticum*. Clin Diagn Lab Immunol 2001: **8**: 522–527.
57. Urban FJ, Moore BS, Breitenbach R. Synthesis of tigogenyl β-*O*-cellobioside heptaacetate and glycoside tetraacetate via Schmidt's trichloroacetimidate method: some new observations. Tetrahedron Lett 1990: **31**: 4421–4424.
58. Westphal O, Lüderitz O, Bister R. Über die Extraction von Bakterien mit Phenol/Wasser. Z Naturforsch (Tiel B) 1952: **7**: 148–155.
59. Wilson M. Biological activities of lipopolysaccharide and endotoxin. In: Haroun HN, ed. Biology of the species *Porphyromonas gingivalis*. Boca Raton, FL: CRC Press, 1993: 171–198.
60. Winkelhoff AJ, Steenbergen TJM, Graaff J. Occurrence and association with disease. In: Haroun HN. ed. Biology of the Species Porphyromonas gingivalis. Boca Raton, Florida: CRC Press, 1993: 33–44.
61. Yamaji Y, Kubota T, Sasaguri K et al. Inflammatory cytokine gene expression in human periodontal ligament fibroblasts stimulated with bacterial lipopolysaccharides. Infect Immun 1995: **63**: 3576–3581.
62. Zeigler-Heitbrock HW, Thiel E, Futterer A, Herzog V, Wirtz A, Riethmuller G. Establishment of a human cell line (Mono Mac 6) with characteristics of mature monocytes. Int J Cancer 1988: **41**: 456–461.

RESEARCH ARTICLE

MyD88-induced downregulation of IRAK-4 and its structural requirements

Fumihiko Hatao[1,2], Maya Yamamoto[2], Masashi Muroi[2], Michio Kaminishi[1] & Ken-ichi Tanamoto[2]

[1]Department of Metabolic Care and Gastrointestinal Surgery, Graduate School of Medicine, The University of Tokyo, Tokyo, Japan; and [2]Division of Microbiology, National Institute of Health Sciences, Tokyo, Japan

Correspondence: Ken-ichi Tanamoto, Division of Microbiology, National Institute of Health Sciences, 1-18-1 Kamiyoga, Setagaya, Tokyo 158-8501, Japan. Tel.: +81 3 3700 1141, ext. 272; fax: +81 3 3707 6950; e-mail: tanamoto@nihs.go.jp

Received 7 February 2008; revised 2 April 2008; accepted 9 April 2008.
First published online 23 May 2008.

DOI:10.1111/j.1574-695X.2008.00425.x

Editor: Patrick Brennan

Keywords
Toll-like receptor; IL-1 receptor; NF-κB.

Abstract

IRAK-4 plays an essential role in Toll-like receptor (TLR)/IL-1 receptor signaling. However, its signaling and regulation mechanisms have remained elusive. We have reported previously that stimulation of TLR2, TLR4 or TLR9, but not TLR3, leads to downregulation of IRAK-4 protein. Here, we show that expression of MyD88 leads to downregulation of endogenous as well as exogenously expressed IRAK-4 protein in HEK293 cells. Expression of TRIF did not cause IRAK-4 downregulation although it induced NF-κB activation. Expression of either a deletion mutant of MyD88 lacking its death domain or MyD88s, neither of which induced NF-κB activation, did not lead to IRAK-4 downregulation. MyD88-induced downregulation was observed in an IRAK-4 mutant lacking the kinase domain, but not in another mutant lacking the death domain. These results demonstrate that downregulation of IRAK-4 requires activation of the MyD88-dependent pathway and that the death domains of both MyD88 and IRAK-4 are important for this downregulation.

Introduction

Toll-like receptor (TLR)/IL-1 receptor (IL-1R) family members share common intracellular signaling proteins including MyD88, IL-1R-associated kinase (IRAK) family and TRAF6 (Fujihara *et al.*, 2003; Janssens & Beyaert, 2003). Ligand binding to TLR/IL-1R triggers the recruitment of adaptor proteins, such as MyD88 and TRIF, to the Toll/IL-1 receptor (TIR) domain of TLR/IL-1R via a homophilic TIR–TIR interaction, which in turn recruits IRAK-4 and IRAK-1 into the receptor complex. IRAK-4 does not bind IRAK-1 directly but is recruited into the complex through binding with MyD88. This allows IRAK-1 and IRAK-4 to come in close proximity, which induces IRAK-4 to phosphorylate IRAK-1 (Li *et al.*, 2002). The phosphorylated IRAK-1 interacts with TRAF6, leading to the activation of NF-κB (Cao *et al.*, 1996).

IRAK-4 plays an essential role in TLR/IL-1R signaling. Residual activation of NF-κB in response to IL-1 is still observed in IRAK-1-deficient cells (Kanakaraj *et al.*, 1998; Thomas *et al.*, 1999). In contrast, almost no response to TLR/IL-1R stimulation is observed in IRAK-4-deficient mice (Suzuki *et al.*, 2002) or in patients with IRAK-4 mutations (Picard *et al.*, 2003; Medvedev *et al.*, 2005). Although IRAK-4 is known to phosphorylate IRAK-1 (Li *et al.*, 2002), the requirement of its kinase activity is still controversial (Lye *et al.*, 2004; Qin *et al.*, 2004). In addition, although the internal regions of MyD88 located between its C-terminal TIR and N-terminal death domains have been reported to be necessary for the interaction with IRAK-4 (Burns *et al.*, 2003), the signaling mechanism and the regulation of IRAK-4 have remained elusive. We have reported previously that prolonged stimulation of TLR2, TLR4 or TLR9 leads to downregulation of IRAK-4 protein (Hatao *et al.*, 2004). In this study, we found that expression of MyD88 led to downregulation of IRAK-4 and analyzed the structural requirements of IRAK-4 for this downregulation.

Materials and methods

Cell culture and reagents

The HEK293 cell line (obtained from the Human Science Research Resources Bank, Tokyo, Japan) was grown in Dulbecco's modified Eagle's medium (Invitrogen, Carlsbad, CA) supplemented with 10% (v/v) heat-inactivated fetal calf

serum (Invitrogen), penicillin (100 U mL^{-1}) and streptomycin (100 μg mL^{-1}). An antiserum against EIAV-tag epitope (amino acid sequence: ADRRIPGTAEE) was a kind gift from Dr Nancy Rice (NCI-Frederick Cancer Research and Development Center). An antibody against β-actin (AC-15) was obtained from Sigma-Aldrich (St Louis, MO).

Plasmids

The coding region of human MyD88 was amplified by reverse transcriptase (RT)-PCR from total RNA prepared from human spleen (OriGene Technologies, Rockville, MD). Plasmids containing mouse IRAK-4 (IMAGE: 3995220) and human TRIF (IMAGE: 5180098) were obtained from the Mammalian Gene Collection. Mutations found in the IRAK-4 and TRIF plasmids were corrected by PCR-mediated mutagenesis. The coding regions of all constructs described above were subcloned into mammalian expression vectors containing the N-terminal EIAV-tag or the FLAG-tag sequence. NF-κB-dependent luciferase reporter plasmid pELAM-L was described previously (Muroi *et al.*, 2002). All mutant plasmids were created by PCR-mediated mutagenesis and mutations were confirmed by DNA sequencing.

NF-κB reporter assay and immunoblotting

The NF-κB-dependent luciferase reporter assay was performed as described elsewhere (Muroi & Tanamoto, 2002). Briefly, HEK293 cells (2–5 × 10^5 cells) were plated in six-well plates and on the following day transfected by the calcium phosphate precipitation method with indicated plasmids, together with 0.2 μg of pELAM-L and 5 ng of phRL-TK (Promega, Madison, WI) for normalization. At 24–32 h after transfection, cellular extracts were prepared by adding a lysis buffer (10 mM HEPES–KOH, pH 7.9, 10 mM KCl, 5 mM EDTA, 40 mM β-glycerophosphate, 0.5% NP-40, 30 mM NaF, 1 mM Na_3VO_4, 1 mM DTT, 100 nM okadaic acid) containing a protease inhibitor cocktail (Roche Diagnostics, Mannheim, Germany). The reporter gene activity was measured using a portion of the cellular extract according to the manufacturer's (Promega) instruction. Another portion of the cellular extract was subjected to sodium dodecyl sulfate-polyacrylamide gel electrophoresis (SDS-PAGE). Proteins were transferred to a polyvinylidene difluoride membrane (Immobilon-P; Millipore, Bedford, MA) and subjected to immunoblotting with the indicated antibodies. The signals were visualized using an enhanced chemiluminescence system (Amersham Biosciences, Piscataway, NJ).

Results

Expression of MyD88 leads to downregulation of IRAK-4

We have already reported that prolonged stimulation of TLR2, TLR4 or TLR9, but not TLR3, leads to downregulation of IRAK-4 protein (Hatao *et al.*, 2004). It is well known that signaling through these TLRs, with the exception of TLR3, involves the adaptor protein MyD88, and expression of MyD88 leads to the activation of NF-κB. Therefore, we transfected an increasing amount of MyD88 expression plasmid together with an NF-κB-dependent reporter plasmid in HEK293 cells and detected IRAK-4 protein (Fig. 1). The protein level of endogenous IRAK-4 decreased in proportion to the amount of MyD88 plasmid transfected (top panel) although the level of β-actin was not affected (third panel from the top). Expression of either a dominant-negative mutant (MyD88-DN; amino acids 135–296) or a splicing variant (MyD88s; lacks amino acids 110–154) of MyD88, neither of which induced NF-κB activation

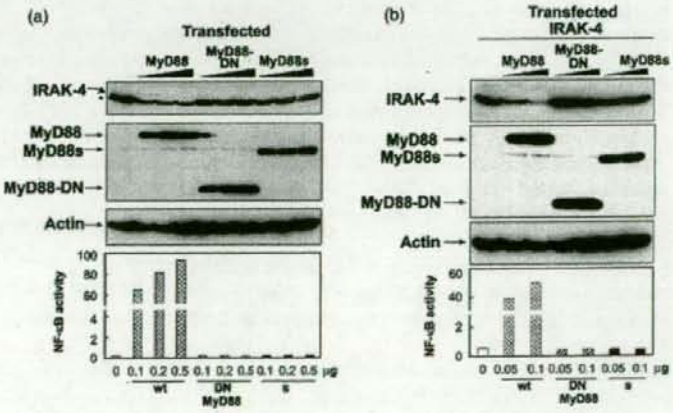

Fig. 1. MyD88-induced downregulation of IRAK-4. An increasing amount of expression plasmid for either EIAV-tagged MyD88, EIAV-tagged MyD88-DN (amino acids 135–296) or EIAV-tagged MyD88s (lacking amino acids 110–154) and an NF-κB-dependent luciferase reporter plasmid were transiently transfected without (a) or with (b) an expression plasmid for EIAV-tagged IRAK-4 into HEK293 cells. After 30 h, cellular extracts were subjected to luciferase activity measurements (bottom panels) and SDS-PAGE, followed by immunoblotting for the detection of endogenous IRAK-4 (a, top panel), EIAV-tagged IRAK-4 (b, top panel), EIAV-tagged MyD88 and its mûtants (second panels) or endogenous β-actin (third panels). The asterisk in the top panel of (a) indicates a nonspecific band.

(bottom panel), did not lead to the decrease in IRAK-4 protein (top panel), although these proteins were expressed properly (second panel from the top). To confirm this, we expressed EIAV-tagged IRAK-4 together with an increasing amount of MyD88, MyD88-DN or MyD88s and detected EIAV-tagged IRAK-4 with an anti-EIAV antibody (Fig. 1b). Exogenously expressed IRAK-4 was also decreased by the expression of MyD88 but not by MyD88-DN or MyD88s (top panel). In this experiment as well, the level of β-actin was not affected (third panel), and MyD88 and all of its mutants were expressed properly (second panel) with the activation of NF-κB by wild-type MyD88 only (bottom panel).

Because stimulation of TLR3 did not lead to downregulation of IRAK-4 (Hatao *et al.*, 2004), and another adaptor protein TRIF is involved in TLR3-mediated signaling, we next asked whether expression of TRIF affects the level of IRAK-4 (Fig. 2). We transfected expression plasmids for EIAV-tagged IRAK4 and either MyD88 or TRIF together with an NF-κB-dependent reporter plasmid in HEK293 cells and detected IRAK-4 protein. Although expression of MyD88 and TRIF both activated NF-κB, only MyD88 induced downregulation of IRAK-4, indicating that downregulation of IRAK-4 requires the activation of the MyD88-dependent pathway. The level of β-actin was not affected by expression of these proteins.

Structural requirement of IRAK-4 for MyD88-induced downregulation

We next asked which domain of IRAK-4 is required to undergo MyD88-induced downregulation. IRAK-4 consists of an N-terminal death domain and a C-terminal kinase domain. We created deletion mutants lacking these domains and examined whether expression of MyD88 affects the level of these mutants (Fig. 3). Expression of MyD88 in HEK293 cells led to downregulation of wild-type IRAK-4 and the deletion mutant (dKD) of the kinase domain, indicating that the kinase domain is not necessary for downregulation. However, the IRAK-4 mutant (dDD) lacking the death domain did not undergo downregulation although the MyD88-induced activation of NF-κB was observed at a level

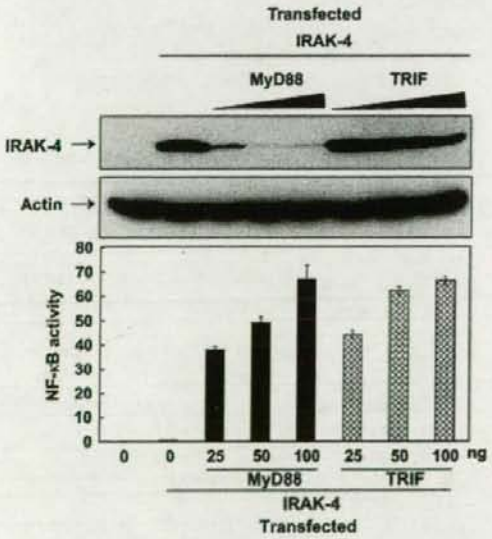

Fig. 2. TRIF does not induce downregulation of IRAK-4. An increasing amount of expression plasmids for either EIAV-tagged MyD88 or EIAV-tagged TRIF and an NF-κB-dependent luciferase reporter plasmid were transiently transfected with an expression plasmid for EIAV-tagged IRAK-4 into HEK293 cells. After 30 h, cellular extracts were subjected to luciferase activity measurements (bottom panel) and SDS-PAGE, followed by immunoblotting for the detection of EIAV-tagged IRAK-4 (top panel) or endogenous β-actin (middle panel). Values are means ± SEM from three independent experiments.

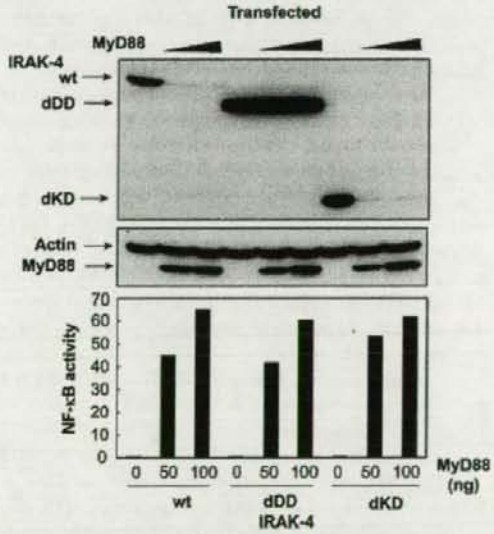

Fig. 3. Structural requirements for IRAK-4 for MyD88-induced downregulation. Each expression plasmid for wild-type (wt) IRAK-4, or an IRAK-4 deletion mutant lacking either death domain (dDD; deletion of amino acids 1–106) or kinase domain (dKD; deletion of amino acids 186–459) was transiently transfected with an increasing amount of EIAV-tagged MyD88 expression plasmid and an NF-κB-dependent luciferase reporter plasmid into HEK293 cells. After 30 h, cellular extracts were subjected to luciferase activity measurements (bottom panels) and SDS-PAGE, followed by immunoblotting for the detection of EIAV-tagged IRAK-4 as well as its mutants (top panel), EIAV-tagged MyD88 and endogenous β-actin (second panels).

comparable to the case when wild-type IRAK-4 was expressed (Fig. 3).

Discussion

We have reported previously that prolonged stimulation of TLR2, TLR4 or TLR9 led to downregulation of IRAK-4 protein whereas the stimulation of TLR3 did not affect the IRAK-4 level (Hatao *et al.*, 2004). MyD88 is involved in signaling through all of these TLRs except TLR3 (Fujihara *et al.*, 2003). Thus, we examined the effect of expression of MyD88 on IRAK-4 protein level and found that expression of MyD88 leads to downregulation of endogenous as well as exogenously expressed IRAK-4 protein (Fig. 1). Our result clearly demonstrates that stimulation of TLRs is not necessary but expression of MyD88 is enough for downregulation of IRAK-4. We used three different IRAK-4 expression plasmids, in which expression of IRAK-4 is controlled by cytomegalovirus (CMV), herpes simplex virus (HSV) thymidine kinase and GAPDH promoters, and IRAK-4 levels expressed through these plasmids were all downregulated by MyD88 (data not shown). In addition, expression of endogenous IRAK-4 is regulated by the promoter different from those described above. It is, therefore, unlikely that the downregulation of IRAK-4 was caused by a decrease in IRAK-4 transcription.

We have reported previously that downregulation of IRAK-4 induced by prolonged stimulation of TLR seems to be mediated through cleavage of IRAK-4 by a protease induced by the activation of NF-κB (Hatao *et al.*, 2004). In this study, MyD88-DN and MyD88s, neither of which induces NF-κB activation, did not lead to IRAK-4 downregulation. On the other hand, expression of TRIF induced a strong activation of NF-κB comparable to MyD88, but also did not cause downregulation (Fig. 2). Therefore, it appears that activation of NF-κB is not enough to induce downregulation of IRAK-4.

An IRAK-4 mutant lacking its death domain did not undergo downregulation, although strong activation of NF-κB was observed upon expression of MyD88 (Fig. 3). This may indicate that a protease that recognizes the death domain is responsible for the downregulation of IRAK-4. We have reported previously that downregulation of IRAK-4 in response to TLR stimulation was not inhibited by broad-spectrum caspase inhibitors (Z-VAD-FMK and A-Asp-CH_2-DCB), a serine protease inhibitor (E-64) and a cathepsin B inhibitor (CA-074 methyl ester), and that the proteasome was unlikely to be involved because a smaller molecular weight protein (*c.* 32 kDa), which appears to be a cleavage product of IRAK-4, was detected by an IRAK-4 antibody following the decrease in IRAK-4 protein (Hatao *et al.*, 2004). We also have not been able to find proteases that specifically recognize the death domain of IRAK-4 using a public protease database (PeptideCutter: http://www.expasy.org/tools/peptidecutter/). Thus, a novel protease or a protease whose recognition sequence has not been identified may be involved in the downregulation of IRAK-4.

An IRAK-4 mutant that lacks the entire kinase domain was downregulated by MyD88, indicating that its kinase domain is not necessary for the downregulation. The involvement of the kinase domain of IRAK-4 in TLR/IL-1R signaling is still controversial (Lye *et al.*, 2004; Qin *et al.*, 2004; Kawagoe *et al.*, 2007; Kim *et al.*, 2007; Koziczak-Holbro *et al.*, 2007). We have reported that downregulation of IRAK-4 in response to TLR stimulation occurred with slower kinetics than the activation of IRAK-1 (Hatao *et al.*, 2004). Thus, a feedback event induced by TLR stimulation seems to be involved in the downregulation. It is well known that prolonged stimulation of a TLR ligand induces a hyporesponsive state to subsequent challenge with ligands for different TLRs (Jacinto *et al.*, 2002; Sato *et al.*, 2002; Dobrovolskaia *et al.*, 2003; Yeo *et al.*, 2003). Because IRAK-4 is essential for signaling through most TLRs (Suzuki *et al.*, 2002), downregulation of IRAK-4 may be involved in the induction of this hyporesponsive state.

Acknowledgements

This research was supported in part by a grant from the Ministry of the Environment.

References

Burns K, Janssens S, Brissoni B, Olivos N, Beyaert R & Tschopp J (2003) Inhibition of interleukin 1 receptor/Toll-like receptor signaling through the alternatively spliced, short form of MyD88 is due to its failure to recruit IRAK-4. *J Exp Med* **197**: 263–268.

Cao Z, Xiong J, Takeuchi M, Kurama T & Goeddel DV (1996) TRAF6 is a signal transducer for interleukin-1. *Nature* **383**: 443–446.

Dobrovolskaia MA, Medvedev AE, Thomas KE, Cuesta N, Toshchakov V, Ren T, Cody MJ, Michalek SM, Rice NR & Vogel SN (2003) Induction of *in vitro* reprogramming by Toll-like receptor (TLR)2 and TLR4 agonists in murine macrophages: effects of TLR "homotolerance" versus "heterotolerance" on NF-κB signaling pathway components. *J Immunol* **170**: 508–519.

Fujihara M, Muroi M, Tanamoto K, Suzuki T, Azuma H & Ikeda H (2003) Molecular mechanisms of macrophage activation and deactivation by lipopolysaccharide: roles of the receptor complex. *Pharmacol Ther* **100**: 171–194.

Hatao F, Muroi M, Hiki N, Ogawa T, Mimura Y, Kaminishi M & Tanamoto K (2004) Prolonged Toll-like receptor stimulation leads to down-regulation of IRAK-4 protein. *J Leukoc Biol* **76**: 904–908.

Jacinto R, Hartung T, McCall C & Li L (2002) Lipopolysaccharide- and lipoteichoic acid-induced tolerance

and cross-tolerance: distinct alterations in IL-1 receptor-associated kinase. *J Immunol* **168**: 6136–6141.

Janssens S & Beyaert R (2003) Functional diversity and regulation of different interleukin-1 receptor-associated kinase (IRAK) family members. *Mol Cell* **11**: 293–302.

Kanakaraj P, Schafer PH, Cavender DE *et al.* (1998) Interleukin (IL)-1 receptor-associated kinase (IRAK) requirement for optimal induction of multiple IL-1 signaling pathways and IL-6 production. *J Exp Med* **187**: 2073–2079.

Kawagoe T, Sato S, Jung A, Yamamoto M, Matsui K, Kato H, Uematsu S, Takeuchi O & Akira S (2007) Essential role of IRAK-4 protein and its kinase activity in Toll-like receptor-mediated immune responses but not in TCR signaling. *J Exp Med* **204**: 1013–1024.

Kim TW, Staschke K, Bulek K *et al.* (2007) A critical role for IRAK4 kinase activity in Toll-like receptor-mediated innate immunity. *J Exp Med* **204**: 1025–1036.

Koziczak-Holbro M, Joyce C, Gluck A, Kinzel B, Muller M, Tschopp C, Mathison JC, Davis CN & Gram H (2007) IRAK-4 kinase activity is required for interleukin-1 (IL-1) receptor- and toll-like receptor 7-mediated signaling and gene expression. *J Biol Chem* **282**: 13552–13560.

Li S, Strelow A, Fontana EJ & Wesche H (2002) IRAK-4: a novel member of the IRAK family with the properties of an IRAK-kinase. *Proc Natl Acad Sci USA* **99**: 5567–5572.

Lye E, Mirtsos C, Suzuki N, Suzuki S & Yeh WC (2004) The role of interleukin 1 receptor-associated kinase-4 (IRAK-4) kinase activity in IRAK-4-mediated signaling. *J Biol Chem* **279**: 40653–40658.

Medvedev AE, Thomas K, Awomoyi A, Kuhns DB, Gallin JI, Li X & Vogel SN (2005) Expression of IL-1 receptor-associated kinase-4 (IRAK-4) proteins with mutations identified in a patient with recurrent bacterial infections alters normal IRAK-4 interaction with components of the IL-1 receptor complex. *J Immunol* **174**: 6587–6591.

Muroi M & Tanamoto K (2002) The polysaccharide portion plays an indispensable role in *Salmonella* lipopolysaccharide-induced activation of NF-κB through human Toll-like receptor 4. *Infect Immun* **70**: 6043–6047.

Muroi M, Ohnishi T & Tanamoto K (2002) MD-2, a novel accessory molecule, is involved in species-specific actions of *Salmonella* lipid A. *Infect Immun* **70**: 3546–3550.

Picard C, Puel A, Bonnet M *et al.* (2003) Pyogenic bacterial infections in humans with IRAK-4 deficiency. *Science* **299**: 2076–2079.

Qin J, Jiang Z, Qian Y, Casanova JL & Li X (2004) IRAK4 kinase activity is redundant for interleukin-1 (IL-1) receptor-associated kinase phosphorylation and IL-1 responsiveness. *J Biol Chem* **279**: 26748–26753.

Sato S, Takeuchi O, Fujita T, Tomizawa H, Takeda K & Akira S (2002) A variety of microbial components induce tolerance to lipopolysaccharide by differentially affecting MyD88-dependent and -independent pathways. *Int Immunol* **14**: 783–791.

Suzuki N, Suzuki S, Duncan GS *et al.* (2002) Severe impairment of interleukin-1 and Toll-like receptor signalling in mice lacking IRAK-4. *Nature* **416**: 750–756.

Thomas JA, Allen JL, Tsen M, Dubnicoff T, Danao J, Liao XC, Cao Z & Wasserman SA (1999) Impaired cytokine signaling in mice lacking the IL-1 receptor-associated kinase. *J Immunol* **163**: 978–984.

Yeo SJ, Yoon JG, Hong SC & Yi AK (2003) CpG DNA induces self and cross-hyporesponsiveness of RAW264.7 cells in response to CpG DNA and lipopolysaccharide: alterations in IL-1 receptor-associated kinase expression. *J Immunol* **170**: 1052–1061.

Food Additives and Contaminants
Vol. 25, No. 10, October 2008, 1283–1290

Taylor & Francis
Taylor & Francis Group

Migration of lactic acid, lactide and oligomers from polylactide food-contact materials

M. Mutsuga*, Y. Kawamura and K. Tanamoto

National Institute of Health Sciences, Tokyo, Japan

(*Received 11 October 2007; final version received 27 February 2008*)

Polylactide (PLA) is used for manufacturing lunch boxes and for packaging fresh food in Japan. PLA can be hydrolysed relatively easily to produce lactic acid, lactide and oligomers. Different types of PLA sheet were subjected to migration tests under various conditions and the lactic acid, lactide and oligomers contents of the migration solutions were determined using liquid chromatography/mass spectrometry (LC/MS). Furthermore, the change in molecular weight was determined by a migration test. PLA was stable at 40°C for 180 days; the total of lactic acid, lactide and oligomers migration levels were 0.28–15.00 $\mu g\,cm^{-2}$. PLA decomposed clearly at 60°C for only 10 days, the total migration levels were increased to 0.73–2840 $\mu g\,cm^{-2}$. PLA sheets with a high D-lactic acid content decomposed particularly rapidly. The amounts of alkali decomposition products, based on the conversion of lactide and oligomers to lactic acid by alkali hydrolysis, corresponded with the total migration levels.

Keywords: alkali decomposition products; lactic acid; lactide; molecular weight; oligomers; polylactide

Introduction

Polylactide (PLA) is used for manufacturing lunch boxes and for packaging fresh food in Japan. Therefore, PLA may be in contact with various type of food. It is produced by the polymerization of lactic acid or lactide (a cyclic dimer), which are mainly supplied from corn starch. PLA can be hydrolysed relatively easily to produce lactic acid, lactide and oligomers, which are subsequently decomposed into water and carbon dioxide by microorganisms (Tuominen 2002).

In the USA two types of PLA with D-lactic acid contents of 6% or less and between 6% and 16%, respectively, are permitted under the Food Contact Notification (FCN) system. In the European Union, lactic acid is registered on the list of monomers and other starting substances in European Directive 2002/72/EC (European Commission 2002).

Due to its biodegradability, there are concerns about the migration products of PLA, which might include lactic acid, lactoyl-lactic acid (a linear dimer), lactide and oligomers. With regard to lactic acid toxicity, the Joint FAO/WHO Expert Committee on Food Additives (JECFA) recommended that neither D-lactic acid nor (DL)-lactic acid should be used in infant foods (World Health Organization (WHO) 1974). The toxicity of lactide was previously investigated by two- and 13-week studies on beagles. The findings revealed the presence of gross and microscopic lesions indicative of irritation, and suggested a no observed adverse effect level (NOAEL) of 100 $mg\,kg^{-1}$ body weight day^{-1} (Hebert et al. 1999). Based on these data, the Food Safety Commission of Japan settled on an acceptable daily intake (ADI) of lactide of 0.1 $mg\,kg^{-1}\,day^{-1}$.

In a previous paper we reported the basic properties of PLA which are relative viscosity, molecular weight, D-lactic acid contents and metal content. Furthermore, we performed overall migration tests on several types of PLA sheet, which gave results of less than 20 $\mu g\,cm^{-2}$, although the values increased under acidic or high-temperature conditions (Mutsuga et al. 2007). Lactic acid and lactide were not included in these residues because they evaporated under the test conditions during heating at 105°C.

Lactide is gradually decomposed to lactic acid under water-rich conditions, and oligomers also supply lactic acid through lactide. When the lactide migration level from PLA is examined, it is also necessary to measure simultaneously the lactic acid and oligomers in migration solution, and to consider them as these total amounts. The current study revealed the presence of lactic acid, lactide and oligomers in PLA migration solutions using liquid chromatography/mass spectrometry (LC/MS). In addition, the molecular weights of the PLA sheets were measured after the migration tests, and the degradation of the PLA was clarified.

*Corresponding author. Email: mutsuga@nihs.go.jp

ISSN 0265-203X print/ISSN 1464-5122 online

DOI: 10.1080/02652030802017529
http://www.informaworld.com

Materials and methods

Sample materials

Four types of PLA sheet (from two different manufacturers) were used in this study. Their properties reported in a previous paper (Mutsuga et al. 2007) are summarized in Table 1.

Reagents

L-lactic acid (98%) was purchased from Sigma-Aldrich Inc. (St Louis, MO, USA). Lactide (3,6-dimethyl 1,4-dioxane-2,5-dione) (98%) was purchased from Aldrich Chemical Co., Inc. (Milwaukee, WI, USA). Formic acid was purchased from Sigma-Aldrich Japan (Tokyo, Japan). High-performance liquid chromatography (HPLC)-grade acetonitrile was purchased from Merck Co., Inc. (Darmstadt, Germany). Water was purified by the Milli-Q SP system (Millipore Co., MA, USA). Sterilized water was prepared for the migration test by autoclaving.

Migration test

The PLA sheets were cut into 2 × 12.5 cm test samples. The test samples were placed into each glass tubes (24 mm i.d. × 220 mm) containing 100 ml of simulant (water, 4% acetic acid or 20% ethanol) and stopper the tubes. The sample tubes were replaced in the thermostatically controlled oven setting at each test temperature, and left for each test period. After their test periods each test sample was removed from simulant. The stimulant was analysed for lactic acid, lactide and oligomers by LC/MS. If the migrant level of lactic acid or lactide were under determination limit ($0.4\,\mu g\,cm^{-2}$), a ten-fold concentration of the migration solution was determined again, which was prepared by dissolving the freeze-dried residue of 10 ml migration solution in 1 ml water.

The migration into heptane at 25°C for 1 h was performed. For the determination of lactic acid, a 10 ml migration solution was transferred to a separatory funnel and added 10 ml water. The water layer injected to LC/MS. Lactide was determined directly by gas chromatography-mass spectrometry (GC/MS) following with the condition of the previous report (Mutsuga et al. 2007).

Measurements of lactic acid, lactide and oligomers

The calibration curves for lactic acid and lactide determination were prepared each in a range of $0.2–5.0\,\mu g\,ml^{-1}$ ($0.4–20\,\mu g\,cm^{-2}$), each correlations were $R^2 > 0.99$. The levels of oligomers (from trimer to 13-mer) were estimated as lactide using the lactide calibration curve and they were then summed. The summation of lactic acid, lactide and oligomers was expressed as total migration level.

LC/MS conditions

The standard or test solution (20 µl) was injected into a LC/MS system (1100 series Agilent Technologies, Palo Alto, CA, USA) under the following conditions; LC column: TSKgel ODS-80TS QA (4.6 mm i.d. × 150 mm; Tosoh Co., Tokyo, Japan), column temperature: 40°C, flow rate: $0.3\,ml\,min^{-1}$, mobile phase: 0–30 min gradient from acetonitrile/0.1% formic acid (1:99) to acetonitrile and 30–40 min acetonitrile, MS electrospray capillary voltage: 3 kV, cone voltage: 60 V, drying gas temperature: 350°C, flow rate: $12\,l\,min^{-1}$ (N_2), ionization mode: electrospray ionization (negative), monitoring mode: selected ion monitoring (SIM), quantitative ion: m/z 89 (lactic acid), 161 (lactide) and $72n+17$ (where oligomers $n = 3–13$).

Measurement of alkali decomposition products

The migration solution of water and 20% ethanol (1 ml) was saponified with 100 µl of 0.2 M sodium hydroxide, followed by heating for 15 min in a water bath at 60°C. After cooling, 100 µl of 0.2 M hydrochloride were added. The lactic acid in the solution was analysed by LC/MS. The calibration curve was produced by treating the lactic acid standard solutions in the same way. The 4% acetic acid migration solution (1 ml) was freeze-dried, and dissolved in 1 ml water and followed above. The amount of total lactic acid obtained by this operation was expressed as the alkali decomposition value.

Measurement of molecular weight

The test sheets were dried at room temperature. A 100-mg sample of each test sheet was dissolved

Table 1. Characterization of PLA sheets used in migration studies.

Sample	Manufacture	Thickness (mm)	Colour	Molecular weight (Mp)	Ratio of D-lactic acid (%)	Free lactide content ($\mu g\,g^{-1}$)
1	A	0.5	Colourless	1.8×10^5	<1.0	252
2	B	0.7	Colourless	1.7×10^5	1.3	1081
3	B	0.7	Colourless	1.7×10^5	4.1	1201
4	B	0.7	Colourless	1.9×10^5	11.3	1567

in 1 ml dichloromethane, and diluted to 25 ml with tetrahydrofuran (THF). Each solution was then subjected to gel-permeation chromatography (GPC). The relative molecular weight at peak top (Mp) were measured using the retention time by reference to a polystyrene standard from Mw 5×10^4 to 4.27×10^5 (TSK standard POLYSTYRENE, A-500, 1000, 2500, 5000, F-1, 2, 4, 10, 20, 40; Tosoh Co.). The GPC conditions were as follows: column: TSK-GEL G4000HXL (7.8 mm i.d. × 300 mm; Tosoh), column temperature: 40°C, mobile phase: THF, flow rate: 1 ml min^{-1}, injection volume: 50 µl, detection: ultraviolet (210 nm).

Results and discussion

Measurements of migrants

In a previous paper (Mutsuga et al. 2007), lactide was measured by GC/MS, but lactic acid and oligomers could not be measured. Therefore, lactic acid, lactide and oligomers in the migration solutions were determined simultaneously by LC/MS.

When the migration solution at 60°C for 5 days was measured in the SCAN mode, some peaks besides lactic acid and lactide were detected. They had m/z $72n+17$ (where $n=3$–13) as a base ion. When the alkali hydrolysis was performed, we only obtained lactic acid. Therefore, these peaks were identified with the oligomers. The chromatograms and mass spectra are shown in Figure 1.

The quantifications were performed in the SIM mode using m/z 89 $[M-H]^-$ for lactic acid, m/z 161 $[M+OH]^-$ for lactide and m/z $72n+17$ (where $n=$ 3–13) $[M-H]^-$ for oligomers. Oligomers could be detected from trimer to 13-mer. Each oligomer was determined using the lactide calibration curve, and the total quantities were calculated. The determination limit of each migrant was 0.04 µg cm^{-2} in ten-fold concentrated migration solution.

It is known that lactide and oligomers decompose easily to lactic acid, and this has been reported for the determination of migrants from PLA with the conversion from lactide and oligomers to lactic acid by alkali hydrolysis as the total amount of alkali decomposition products (Conn et al. 1995). The rate of decomposition of lactide solution (400 µg ml^{-1}) was 96.0%. In the migration solution shown in Figure 1a, the lactide and oligomers had completely decomposed to lactic acid (Figure 1b).

Stability of lactic acid and lactide in the simulants

Lactide is hydrolysed to lactic acid, which is then converted to water and carbon dioxide by microorganisms. Thus, it was important to consider the reduction of lactic acid and lactide during the migration test and the preservation before analysis. The stabilities of the compounds were confirmed using 1 µg ml^{-1} solution under the migration test conditions. Migration tests were performed with water, 4% acetic acid and

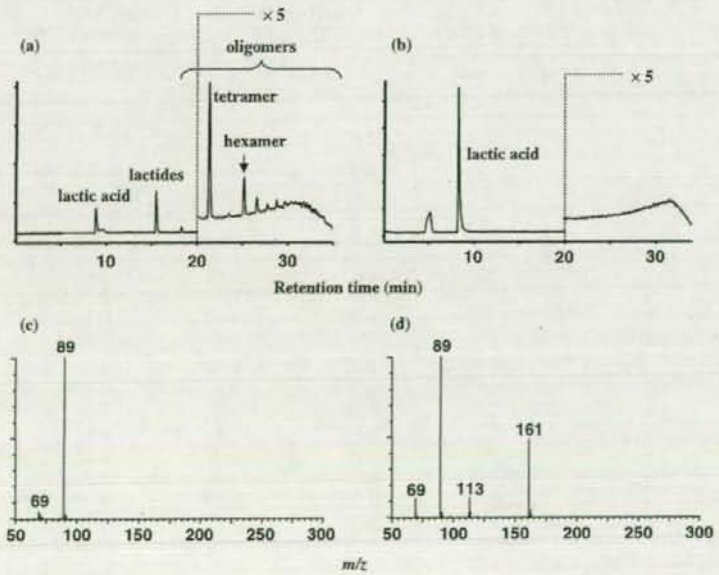

Figure 1. LC/MS/total ion chromatograms of migration solution from sample 3 at 60°C for 5 day into water (a) and after alkali hydrolysis (b), and mass spectra of lactic acid (c) and lactide (d).

20% ethanol as food simulants. Acetic acid is a simulant for acidic foods. Polylactide is polyester resin, and polyester is weak to alcohol. Therefore, 20% ethanol which is a simulant for liquor was also tested.

Lactic acid was stable under all of the test conditions, remaining at 86.6% even after incubation at 60°C for 10 days (Table 2). Lactide remained at 98.5–103.3% when incubated at 60°C for 30 min in each simulant, but the residual ratios were reduced to 73.0% and 21.0% after 1 and 10 days, respectively. By contrast, lactic acid was detected in these solutions at levels corresponding to the reduction of lactide. Thus, the lactide appeared to have been converted to lactic acid. This process also occurred on the oligomers which were converted to lactic acid via lactide. Therefore, it should be necessary to consider that migrants of lactide are as total of lactic acid, lactide and oligomers.

Effect of simulants and temperature in the short-term migration test

Migration tests were performed on four types of PLA sheet in water, 4% acetic acid and 20% ethanol at 60°C for 30 min. The migration levels of lactic acid, lactide, oligomers and alkali decomposition products were measured (Table 3). Lactic acid migration was detected at levels of 0.06–0.40 $\mu g\,cm^{-2}$ from all of the samples into water, 4% acetic acid and 20% ethanol. The highest level of lactic acid migration was observed in 4% acetic acid. The lactide migration was ranging from not determined (n.d.) to 2.4 $\mu g\,cm^{-2}$ and highest into 20% ethanol. Lactide migration was detected from samples 2–4, with sample 4 showing particularly high levels. By contrast, sample 1 showed little or n.d. lactide migration. Oligomers migration was detected only from samples 3 and 4 into 20% ethanol at 60°C for 30 min. However, sample 4 showed high levels of lactide migration into each type of simulant, particularly into 20% ethanol, which showed high migration levels and the presence of oligomers. With heptane at 25°C for 1 h, lactic acid and lactide were not detected from all of the samples.

The effect of the migration temperature was studied using sample 3 at 20, 40, 60, 80 and 95°C for 30 min (Table 4). The migration levels of lactic acid did not change at temperatures from 20°C to 80°C, and increased slightly at 95°C. While, the migration levels of lactide were increased to 0.24 $\mu g\,cm^{-2}$ at 60°C, to 0.64 $\mu g\,cm^{-2}$ at 80°C and to 4.12 $\mu g\,cm^{-2}$ at 95°C. Oligomers were detected at 1.98 $\mu g\,cm^{-2}$ only at 95°C. The sample became clouded after the migration test at 95°C.

Table 2. Stability of lactic and lactide under various conditions.

	Water			4% Acetic acid	20% Ethanol
	60°C, 30 min	60°C, 1 day	60°C, 10 day	60°C, 30 min	60°C, 30 min
Lactic acid	101.5±2.0	94.1±3.8	86.6±4.0	116.5±4.0	102.6±1.8
Lactide	99.4±1.7	73.0±2.6	21.0±6.0	98.7±0.2	103.3±1.5

Notes: Values are the mean (%) ± SD of three trials.
All trials each used 1 $\mu g\,ml^{-1}$ standard solution.

Table 3. Comparison of simulant in short-term test (60°C, 30 min).

		Level ($\mu g\,cm^{-2}$)				
Simulant	Sample	Lactic acid	Lactide	Oligomers	Total	Alkali decomposite
Water	1	0.12	n.d.	n.d.	0.12	0.18
	2	0.22	0.17	n.d.	0.43	0.45
	3	0.23	0.24	n.d.	0.53	0.68
	4	0.19	0.97	n.d.	1.40	1.63
4% Acetic acid	1	0.08	n.d.	n.d.	0.08	0.28
	2	0.34	0.19	n.d.	0.58	0.53
	3	0.35	0.30	n.d.	0.72	0.73
	4	0.40	1.22	n.d.	1.92	1.78
20% Ethanol	1	0.13	0.07	n.d.	0.22	0.33
	2	0.23	0.41	n.d.	0.74	0.93
	3	0.23	0.84	0.20	1.53	1.78
	4	0.24	2.41	1.16	4.70	5.18

Notes: Values are the mean of two trials.
n.d.:<0.04.
The oligomers (from trimer to 13mer) were measured as lactide.
Total = (lactic acid) + (lactide + oligomers) × 1.25, calculated as lactic acid.

PLA hydrolysis has been reported to accelerate rapidly at temperatures above the glass-transition point of 55–60°C (Marcelo and James 1992; Conn et al. 1995). PLA decomposition appeared to have occurred at 60°C or more with the increasing of lactide levels (Table 4). However, the lactic acid levels did not alter from 20°C to 80°C. At 95°C, lactic acid was estimated to be produced from lactide generated by PLA decomposition.

Long-term migration into water at 40°C

The migration into water at 40°C was compared during 1, 3 and 6 months. The molecular weights of the tested samples were also measured. The levels of lactic acid, lactide, oligomers, alkali decomposition products and molecular weight are shown in Table 5.

Table 4. Effect of temperature on migrants from sample 3 into water.

	Level ($\mu g\,cm^{-2}$)			
Temperature (°C)	Lactic acid	Lactide	Oligomers	Total
20	0.24	n.d.	n.d.	0.24
40	0.24	n.d.	n.d.	0.24
60	0.22	0.24	n.d.	0.52
80	0.20	0.64	n.d.	1.00
95	0.36	4.12	1.98	7.99

Notes: Values are the mean of two trials.
n.d.:<0.04.
The oligomers (from trimer to 13mer) were measured as lactide.
Total = (lactic acid) + (lactide + oligomers) × 1.25, calculated as lactic acid.

Lactic acid was detected from all of the samples. However, the levels were generally less than $2\,\mu g\,cm^{-2}$ and the highest was $3.88\,\mu g\,cm^{-2}$ for sample 3 after 6 months. Lactide was detected from samples 2–4, and the levels were from n.d. to $0.24\,\mu g\,cm^{-2}$. Oligomers was detected only in samples 2–4 after 6 months. The total migrants were less than $1\,\mu g\,cm^{-2}$ after 6 months for most of the samples, though samples 3 and 4 were 9.00 and $14.66\,\mu g\,cm^{-2}$, which were similar to the short-term migration levels at 60°C for 30 min.

The main compound detected in the long-term tests was lactic acid. This was attributed to the fact that lactide and oligomers generated from PLA had decomposed to lactic acid during the test periods.

To clarify further the polymer decomposition, the molecular weights of the samples after the migration tests were measured. The Mp of the samples before the migration tests ranged from 1.7×10^5 to 1.9×10^5 (Table 1). The values after the migration tests are shown in Table 5. The molecular weights of samples 1–4 decreased to 1.1×10^5 to 1.6×10^5 after 3 months, and to 5.3×10^4 to 1.3×10^5 after 6 months. PLA was decomposed even below the glass-transition temperature in water for a long time. Since their Mp decreased by a small amount, it was speculated that decomposition of PLA had occurred by the removing of some lactide units from the terminal of polymer. The GPC chromatograms of samples 3 and 4 (Figure 2) revealed a clear decrease in Mp. Sample 4 showed a particularly notable decrease.

The most migrant levels were less than $1\,\mu g\,cm^{-2}$. PLA was comparatively stable when the PLA was in contact with water at 40°C. But, sample 3 and 4, which had a high D-lactic acid content, had clearly

Table 5. Migration levels into water at 40°C.

		Level ($\mu g\,cm^{-2}$)					
Testing time	Sample	Lactic acid	Lactide	Oligomers	Total	Alkali decomposite	Molecular weight (Mp)
1 Month	1	0.05	n.d.	n.d.	0.05	0.18	1.8×10^5
	2	0.12	n.d.	n.d.	0.12	0.23	1.6×10^5
	3	0.07	0.06	n.d.	0.15	0.43	1.6×10^5
	4	0.57	0.24	n.d.	0.87	0.93	1.7×10^5
3 Month	1	0.10	n.d.	n.d.	0.10	0.25	1.6×10^5
	2	0.23	0.05	n.d.	0.29	0.55	1.3×10^5
	3	0.20	n.d	n.d.	0.20	0.33	1.2×10^5
	4	1.04	0.11	n.d.	1.19	1.28	1.1×10^5
6 Month	1	0.13	n.d.	n.d.	0.13	0.28	1.3×10^5
	2	0.41	0.05	0.22	0.75	0.88	8.9×10^4
	3	3.88	0.08	4.02	9.00	9.93	6.7×10^4
	4	2.41	0.20	9.60	14.66	15.00	5.3×10^4

Notes: Values are the mean of three or four trials.
n.d.:<0.04.
The oligomers (from trimer to 13mer) were measured as lactide.
Total = (lactic acid) + (lactide + oligomers) × 1.25, calculated as lactic acid.

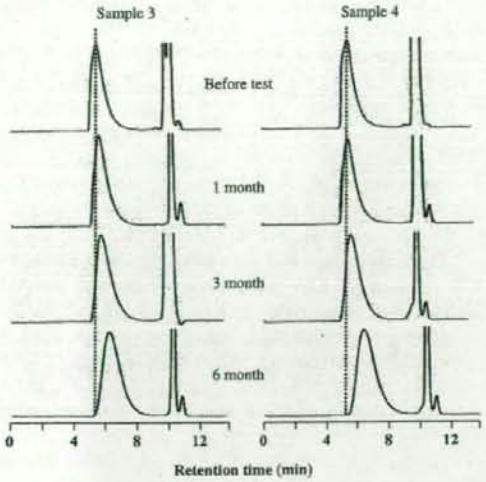

Figure 2. GPC chromatograms of sample 3 and 4 after migration test at 40°C.

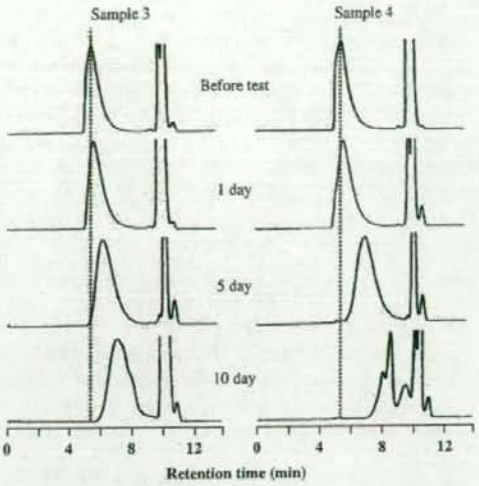

Figure 3. GPC chromatograms of sample 3 and 4 after migration test at 60°C.

Table 6. Migration test into water at 60°C.

Testing time	Sample	Level ($\mu g\,cm^{-2}$)					Molecular weight (Mp)
		Lactic acid	Lactide	Oligomers	Total	Alkali decomposite	
1 Day	1	0.20	0.08	n.d.	0.30	0.30	1.6×10^5
	2	0.13	0.44	n.d.	0.68	0.60	1.5×10^5
	3	0.28	1.08	n.d.	1.63	1.60	1.4×10^5
	4	0.85	5.30	0.46	8.05	8.38	1.4×10^5
5 Day	1	0.29	0.10	n.d.	0.41	0.63	1.4×10^5
	2	0.49	0.22	0.52	1.41	1.60	9.5×10^4
	3	1.70	0.75	1.00	3.89	4.38	6.0×10^4
	4	9.84	6.08	5.74	24.62	27.70	1.9×10^4
10 Day	1	0.60	0.08	n.d.	0.70	0.73	1.0×10^5
	2	2.65	0.22	0.04	2.98	3.55	4.2×10^4
	3	8.78	1.20	0.74	11.20	14.28	1.8×10^4
	4	420	398	1358	2615	2840	4.7×10^3

Notes: Values are the mean of two trials.
n.d.:<0.04.
The oligomers (from trimer to 13mer) were measured as lactide.
Total = (lactic acid) + (lactide + oligomers) × 1.25, calculated as lactic acid.

decomposed by the 6-month migrant test. The decomposition of polymer was correlated with the increase in the migrant levels.

Migration into water at 60°C

The migration test was carried out at 60°C for 30 min, 1, 5, and 10 days in consideration of the case where PLA lunch boxes are kept warm in a hot vendor. The levels of lactic acid, lactide, oligomers and molecular weight are shown in Table 6.

Advanced decomposition was detected far earlier at 60°C than at 40°C, and the migrant levels at 60°C after 1 day were similar to those at 40°C after 6 months. For sample 1, oligomers were not detected even after 10 days, and the total migrants were less than $1\,\mu g\,cm^{-2}$. However, the molecular weights had clearly decreased after 10 days, which suggested that decomposition had progressed slowly. For samples 2 and 3 the levels of lactic acid were notably increased, and oligomers migration was detected after 5 days.

Table 7. Migration levels into water at 95°C.

Testing time	Sample	Level ($\mu g\,cm^{-2}$) Lactic acid	Lactide	Oligomers	Total	Alkali decomposite
30 min	1	0.08	0.45	n.d.	0.64	0.85
	2	0.10	2.49	0.76	4.16	4.88
	3	0.37	4.13	1.98	8.00	8.88
	4	1.49	11.81	5.96	23.69	25.28
60 min	1	0.28	0.94	0.10	1.58	1.38
	2	0.88	3.20	0.36	5.33	7.25
	3	1.52	8.08	0.76	12.57	12.70
	4	2.00	15.78	1.24	23.28	32.50
120 min	1	0.44	1.02	0.26	2.04	1.68
	2	1.68	6.56	0.74	10.81	11.73
	3	2.38	10.36	1.18	16.81	19.83
	4	9.88	29.94	1.86	49.63	51.75

Notes: Values are the mean of two trials.
n.d.:<0.04.
The oligomers (from trimer to 13mer) were measured as lactide.
Total = (lactic acid) + (lactide + oligomers) × 1.25, calculated as lactic acid.

The GPC chromatograms of samples 3 and 4 are shown in Figure 3. In particular, the polymer in sample 4 had broken down completely after 10 days, and the dried test sample had lost its elasticity and collapsed easily into a powder form.

Based on these findings, PLA is not suitable for use at temperatures over 60°C for periods of several days, particularly if it contains high D-lactic acid levels.

Migration into water at 95°C

The migration test at 95°C for 30, 60, and 120 min was carried out to mimic the use of lunch boxes in a microwave oven or over 100°C. Both lactic acid and lactide migration were detected from all of the samples, and the levels increased with the testing period (Table 7). Oligomers were detected from samples 2–4 after 30 min, and from sample 1 after 60 min. The migration levels, according to the sum of migrants at 95°C after 30 min, were same as those at 40°C after 6 months and at 60°C after 5 days. The lactide levels were particularly high. Sample 4 showed more migration than the other samples, but it was at a smaller level than at 60°C for 10 days.

Comparison between the summation of the migrants and alkali decomposition product values

The amount of alkali decomposition products were almost similar to total of lactic acid, lactide and oligomers. The quantities of alkali decomposition products produced were usually higher than the total migration. This difference was attributed to three factors: the fact that the oligomers were determined by a lactide calibration curve, the presence of oligomers at levels less than the determination limit, and the presence of oligomers larger than 14-mers.

Conclusions

The main migrants from PLA were lactic acid, lactide and oligomers. It is necessary for the stability and food safety of PLA to measure the total lactic acid, lactide and oligomers because PLA easily decomposes to oligomers, then to lactide and lactic acid. But these were not included in the overall migration test residues. In this paper the migrants were measured using two measuring methods: total migration and alkali decomposition products. We obtained almost the same results.

PLA was relatively stable at 40°C over 6 months. However, at 60°C or above the glass-transition temperature the polymer was decomposed and the migrant levels increased. This tendency was particularly notable in PLA that contained high D-lactic acid levels. Moreover, the PLA products should be chosen for their purpose according to the prevailing conditions.

References

Conn RE, Kolstad JJ, Borzelleca JF, Dixler DS, Filer Jr LJ, LaDu Jr BN, Pariza MW. 1995. Safety assessment of polylactide (PLA) for use as food-contact polymer. Food Chem Toxicol. 33:273–283.

European Commission. 2002. Commission Directive 2002/72/EC of 6 August 2002 relating to plastic materials and articles intended to come into contact with foodstuffs. Off J Eur Comm. L 220:18–58.

Hebert CD, Giles HD, Heath JE, Hogan DB, Modderman JP, Conn RE. 1999. Toxicity of lactide in

dog after 2 and 13 weeks of daily oral dosing. Food Chem Toxicol. 37:335–342.

Marcelo O, James M. 1992. The influence of polymer glass transition temperature and molecular weight on drug release from tablets containing poly(DL-lactic acid). Pharma Res. 9:26–32.

Mutsuga M, Kawamura Y, Tanamoto K. 2007. Studies on polylactide properties. Jpn J Food Chem. 14:87–92.

Tuominen J, Kylma J, Kapanen A, Venelampi O, Itavaara M, Seppala J, 2002. Biodegradation of lactic acid based polymers under controlled composting conditions and evaluation of the ecotoxicological impact. Biomacromolecules. 3:445–455.

World Health Organization (WHO). 1974. Lactic acid and its ammonium, calcium, potassium and sodium salts. Food Additives Series No. 5. Geneva: WHO.

JOURNAL OF CLINICAL MICROBIOLOGY, Apr. 2008, p. 1169–1173 Vol. 46, No. 4
0095-1137/08/$08.00+0 doi:10.1128/JCM.00856-07

Multiple Combinations of P[13]-Like Genotype with G3, G4, and G5 in Porcine Rotaviruses▽

Wisoot Chan-it,[1] Pattara Khamrin,[3] Prayuth Saekhow,[2] Chansom Pantip,[1] Aksara Thongprachum,[1] Supatra Peerakome,[1] Hiroshi Ushijima,[3] and Niwat Maneekarn[1]*

Department of Microbiology, Faculty of Medicine,[1] and Faculty of Veterinary Medicine,[2] Chiang Mai University, Chiang Mai, Thailand, and Department of Developmental Medical Sciences, Institute of International Health, Graduate School of Medicine, The University of Tokyo, Tokyo, Japan[3]

Received 24 April 2007/Returned for modification 18 June 2007/Accepted 24 January 2008

Epidemiological surveillance of porcine rotavirus (PoRV) strains was carried out in Chiang Mai Province, Thailand, from 2002 to 2003, and eight rotavirus isolates could not be completely typed by PCR. Of these, six were G3 and one was G4 and displayed a P-nontypeable genotype, while another isolate was both G and P nontypeable. Analysis of a partial VP4 gene of all eight P-nontypeable strains revealed a high degree of amino acid sequence identities (94.7% to 100%), suggesting that they belonged to the same P genotype. Comparison of the amino acid sequences of two representative strains (namely, strains CMP178 and CMP213) with those of 27 other known P genotypes revealed a high degree of amino acid sequence identity with those of P[13] porcine rotavirus reference strains HP113 and HP140, which were recently isolated in India. However, amino acid sequence comparison with non-P[13] rotavirus strains revealed relatively low identities, ranging from 58.2% to 84.8% for full-length VP4 sequences and 35.1% to 80.6% for VP8* sequences. Phylogenetic analysis revealed that CMP178 and CMP213 clustered together in a monophyletic branch with P[13]-like genotypes HP113 and HP140 which was clearly separated from the other lineages of P[13] or P[22] strains. Altogether, these findings indicate that PoRV strains CMP178 and CMP213 should be considered the P[13]-like VP4 genotype, a rare genotype that has been identified only in pigs. This study provides additional evidence of increasing genetic diversity among group A rotaviruses in nature.

Group A rotaviruses are the most important etiologic agents of severe diarrhea in young children and young animals worldwide. In developing countries, these severe diarrhea cases lead to an estimated 454,000 to 705,000 deaths annually among children under 5 years of age (32). Group A rotaviruses are members of the *Reoviridae* family with nonenveloped icosahedral particles. The mature virion is formed by three concentric layers of proteins that enclosed a genome of 11 segments of double-stranded RNA. Rotaviruses are classified according to the genetic and antigenic diversity of the two outer capsid proteins, VP4 and VP7. These proteins independently induce type-specific neutralizing antibodies and form the basis of the dual classification of group A rotaviruses into the P (protease sensitive) and the G (glycoprotein) serotypes, respectively (5, 17).

Rotaviruses express extensive antigenic and genomic diversities. To date, at least 15 G genotypes and 26 P genotypes have been identified from humans and a variety of animal species (5, 22, 26, 28, 30, 35, 36). Most recently, several groups of investigators have proposed a novel genotype, P[27], which was isolated from diarrheic piglets (18, 25, 38). Generally, rotaviruses of the same G genotypes share at least 90 to 91% VP7 amino acid sequence identity (11, 12, 13, 16). Rotavirus strains sharing ≥89% VP4 amino acid sequence identities are considered to belong to the same P genotype, while those sharing VP4 amino acid sequence identities of <89% belong to different genotypes (2, 5, 7). Moreover, the VP8* trypsin-cleavage product of VP4 coding for amino acids (aa) 13 to 250, including the greatest sequence divergent region (aa 71 to 204), correlates well with VP4 genotype specificity (20, 21).

Several epidemiological studies have demonstrated that among porcine rotaviruses (PoRVs), G3, G4, and G5, are the most common G genotypes and usually associate with the P[6] or P[7] genotype (5, 23, 39, 40). In addition, other G and P types, such as G1, G2, G6, G8, G9, and G10 and P[13], P[19], P[23], P[26], and P[27], have also been identified in various geographical settings (1, 3, 5, 9, 10, 16, 18, 27, 29, 33, 34, 37, 39, 40, 41). Accordingly, a comprehensive genotypic characterization of the rotavirus strains circulating in domestic animal populations, especially pigs, is important to define the extent of rotavirus diversity.

Rotavirus strains bearing P[13] genotype specificity are host restricted. The P[13] rotavirus genotype is commonly detected among pigs and has not been identified from other animal sources or humans (5, 7, 39, 16). Nevertheless, only a few studies have reported on the distribution of the P[13] genotypes circulating worldwide. Most recently, genome characterization of two PoRV strains, HP113 and HP140, isolated from eastern India revealed that their VP4 sequences were similar to those of P[13] genotypes, while their VP7 sequences were closely related to those of the G6 genotype reference strains (7). In our study, eight strains of P[13] in combination with either G3, G4, or G5 were isolated from diarrheic piglets raised in several farms in Chiang Mai, Thailand. The VP4 genes of these strains were most closely related to those of

* Corresponding author. Mailing address: Department of Microbiology, Faculty of Medicine, Chiang Mai University, 110 Inthawaroros Rd., Sripume, Maung Chiang Mai 50200, Thailand. Phone: 66-53-945332. Fax: 66-53-217144. E-mail: nmaneeka@mail.med.cmu.ac.th.

▽ Published ahead of print on 30 January 2008.

P[13]-like PoRV strains HP113 and HP140. These findings affirm the evidence that rotavirus strains bearing the P[13] genotype are frequently detected in pigs.

MATERIALS AND METHODS

Fecal specimens and rotavirus detection. A total of 250 fecal specimens were collected from diarrheic piglets on six different farms in Chiang Mai, Thailand, in 2002 and 2003. The specimens were evaluated for the presence of group A rotavirus by enzyme-linked immunosorbent assay (ELISA) with a polyclonal antibody against group A rotavirus as the capture antibody (15). The samples that were positive for group A rotavirus by ELISA were investigated further for their G and P genotypes by multiplex reverse transcription-PCR (RT-PCR), as described elsewhere (4, 6, 9, 10, 11, 24, 31, 40).

RNA extraction and RT-PCR genotyping. Viral double-stranded RNA was extracted from a 20% fecal sample suspension with a QIAamp viral RNA mini kit (Qiagen, Hilden, Germany), according to the manufacturer's protocol. For G typing, the VP7 gene was reverse transcribed and amplified by using the consensus primer pair Beg9-End9 (11). Then, the G type was determined by using different pools of primers currently reported to be specific for human and animal G types (G1 to G6 and G8 to G11) (4, 10, 11, 40). For P typing, the consensus primer pair Con2-Con3 was used to generate a 876-bp fragment (VP8*) of VP4, and the P type was determined by using different pools of primers currently reported to be specific for human and animal P types (P[1], P[3] to P[11], P[14], and P[19]) (6, 9, 24, 31, 40).

Nucleotide sequencing. Rotavirus strains that failed to be genotyped by multiple sets of primers were further investigated by nucleotide sequencing. The full-length VP7 (1,062-bp) and partial VP4 (876-bp) genes of these strains were reverse transcribed and were amplified by using the primer pairs Beg9-End9 (10) for VP7 and Con2-Con3 (8) for partial VP4 genes. In addition, the full-length VP4 genes of two representative strains, CMP178 and CMP213, were also amplified by using reverse primer 170 (nucleotides [nt] 2344 to 2368; 5′-GGTCAC AWCCTCTAGMMRYTRCTTA-3′) (26) in combination with forward primer VP4-5F (nt 1 to 23; 5′-GGCTATAAAATGGCTTCDCTCAT-3′). The PCR amplicons were purified with a QIAquick PCR purification kit (Qiagen) and sequenced in both directions by using a BigDye Terminator cycle sequencing kit (Applied Biosystems, Foster City, CA) on an automated sequencer (ABI 3100; Applied Biosystems). For sequencing of the full-length VP4 genes, four additional primers were used as internal sequencing primers. The nucleotide positions and sequences of these primers (5′ to 3′) were as follows: forward primer P28F650, nt 685 to 704, CTTCCACCAATGCAGAATAC; forward primer P28In1, nt 1262 to 1283, CGGATTATGTATCTCTTAACTC; forward primer P28In2, nt 2007 to 2027, GGAGAAATTCATACCAAATAG; and reverse primer P28In3, nt 375 to 396, CACTAGGTTAACTTGTTGA CCG.

Sequences and phylogenetic analysis. The nucleotide sequences were assembled and analyzed by using Bioedit software packages (14). The sequences were compared with those available in the GenBank database by use of the BLAST program in order to determine their genotypes. Phylogenetic and molecular evolutionary analyses were conducted by using the MEGA program (version 3.1) (19). A phylogenetic tree was elaborated by both the parsimony and the distance methods and by supplying statistical support with bootstrapping over 100 replicates.

Nucleotide sequence accession numbers. The full lengths of the VP7 and VP4 gene sequences of strains CMP178 and CMP213 described in this study have been deposited in the GenBank sequence database under accession numbers DQ515961 (VP7) and DQ536362 (VP4) for CMP178 and DQ786576 (VP7) and DQ786578 (VP4) for CMP213.

RESULTS

G and P genotypes. Of a total of 250 fecal specimens tested, 43 (17.2%) were positive for group A rotavirus by ELISA. Characterization of their G and P genotypes by multiplex RT-PCR revealed that 29 isolates were G3, 1 was G4, 4 were G8, 2 were G9, and 7 were G nontypeable. These seven G-nontypeable strains were further characterized by nucleotide sequence analysis, and six were identified to be G3 and 1 was G5. The P genotype was also characterized; and 20 were P[6], 10 were P[7], 5 were P[19], and 8 were P nontypeable. Among these P-nontypeable strains, six were found in combination with G3 (strains CMP213, CMP214, CMP215, CMP225, CMP234, and CMP239), one was found to carry G4 genotype (strain CMP077), while another one was found to be both G and P nontypeable (strain CMP178). Therefore, representative strains CMP178 and CMP213 were selected and their full-length VP4 and VP7 gene sequences were characterized further.

TABLE 1. Comparison of the VP7 deduced amino acid sequence identities of strains CMP178 and CMP213 with the amino acid sequences of 15 known G genotypes

Strain (origin)[a]	G genotype	% VP7 amino acid identity[b]	
		CMP178	CMP213
Wa (human)	1	78.2	80.7
Hu/5 (human)	2	72.3	74.1
YO (human)	3	84.6	**94.4**
AU-1 (human)	3	84.6	**95.4**
P (human)	3	85.5	**95.1**
CP-1 (bovine)	3	85.5	**96.8**
PP-1 (bovine)	3	85.5	**96.8**
A131 (porcine)	3	85.8	**94.7**
A138 (porcine)	3	84.9	**96.0**
4F (porcine)	3	86.1	**95.0**
Gottfried (porcine)	4	74.5	77.2
OSU (porcine)	5	**92.3**	86.0
JL49 (porcine)	5	**92.6**	86.3
H-1 (equine)	5	**92.9**	86.3
A46 (porcine)	5	**92.6**	86.7
134/04-15 (porcine)	5	**93.2**	86.3
NCDV (bovine)	6	81.5	83.5
PO-13 (avian)	7	58.9	56.7
B37 (bovine)	8	78.2	82.5
116E (human)	9	80.9	83.5
B223 (bovine)	10	78.8	81.1
YM (porcine)	11	88.3	86.7
L26 (human)	12	79.4	80.7
L338 (equine)	13	77.6	80.7
CH3 (equine)	14	78.5	84.2
Hg18 (bovine)	15	77.6	77.2

[a] The GenBank accession numbers of the VP7 genes are as indicated for the following strains: Wa, K02033; Hu/5, A01028; YO, D86284; AU-1, D86271; P, AB118024; CP-1, AF448852; PP-1, AF427124; Gottfried, X06386; OSU, X04613; JL49, AY538665; H-1, AF242393; A46, L35054; 134/04-15, DQ062572; NCDV, M12394; PO-13, D82979; B37, J04334; 116E, L14072; B223, X57852; YM, M23194; L26, M58290; L338, D13549; CH3, D25229; and Hg18, AF237666.

[b] Boldface data indicate percentages of the highest sequence identity that CMP178 and CMP213 shared with the corresponding reference genotypes.

VP7 sequence analysis. The deduced amino acid sequences of strains CMP178 and CMP213 were compared with those of representative strains of 15 other known G genotypes. The VP7 amino acid sequence of CMP178 was the most closely related to the amino acid sequences of G5 rotavirus strains, with the amino acid sequence identities ranging from 92.3% to 93.2%, while the VP7 amino acid sequence of CMP213 was the most closely related to the amino acid sequences of the G3 genotypes (94.4% to 96.8%) (Table 1). The data indicated that CMP178 belongs to the G5 genotype and also confirmed that CMP213 has the G3 genotype. Phylogenetic analysis of the deduced amino acid sequences corroborated the results of the analysis of the VP7 sequences by demonstrating that CMP178 and CMP213 clustered with the reference strains of the G5 and G3 rotaviruses, respectively (Fig. 1).

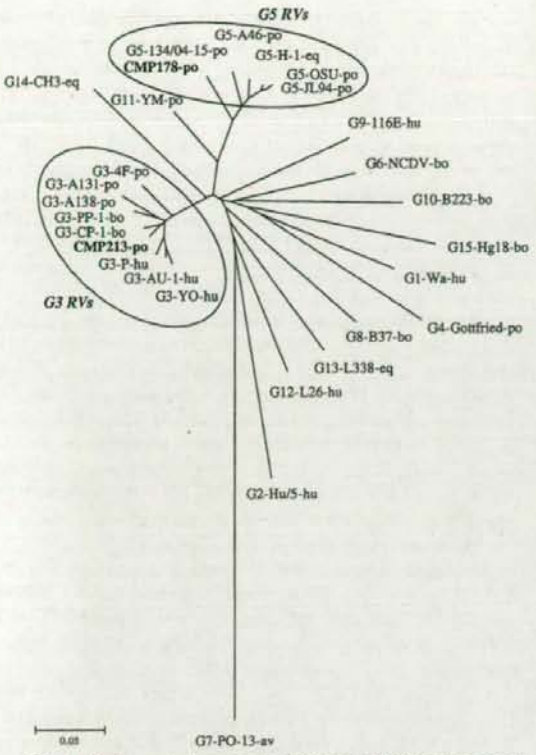

FIG. 1. Phylogenetic tree of the full-length VP7 amino acid sequences displaying the relationships between PoRV strains CMP178, CMP213, and representative strains of all the VP7 genotypes recognized to date. The following abbreviations are used to identify the species of strain origin: hu, human; eq, equine; po, porcine; bo, bovine; av, avian.

VP4 sequence analysis. In order to determine the P genotypes of all eight P-nontypeable PoRV strains, their partial VP4 amplicons (876 bp), which had been generated by the consensus primer pair Con2-Con3, were first subjected to nucleotide sequencing. Comparison of the partial VP4 amino acid sequences of these strains revealed high degrees of amino acid sequence identity (94.7% to 100%) among themselves (data not shown), suggesting that they all belong to the same P genotype.

Analysis of the full-length VP4 amino acid sequences revealed that both representative strains, CMP178 and CMP213, were almost identical (98.4% amino acid identity; data not shown). In addition, when the amino acid sequences of CMP178 and CMP213 were compared with those of 27 known P genotypes (Table 2), the highest level of amino acid sequence identity was found to be with P[13]-like PoRV strains HP113 and HP140 (88.1% and 87.2% for the VP8* portion and 92.2 and 92.4% for the complete VP4 sequences for CMP178 and CMP213, respectively). In contrast, they showed somewhat lower levels of VP8* amino acid sequence identity with other P[13] reference strains, strains MDR-13, JP35-7, JP13-3, ICB2212, ICB2219, and A46, ranging from 79.2% to 83.7% amino acid identity for CMP178 and 79.2% to 83.2% amino acid identity for CMP213. Additionally, they also showed lower levels of amino acid sequence identity with P[22] lapine rotavirus reference strains 160/01, 229/01, 308/01, and 3489/3, ranging from 77.9% to 81.0% for CMP178 and 78.4% to 81.0% for CMP213. Therefore, all eight isolates were considered to be P[13]-like viruses since they had the highest level of sequence identity with P[13] PoRV strains and revealed remarkably lower levels of amino acid sequence identity with

TABLE 2. Comparison of the VP4 and VP8* deduced amino acid sequence identities of strains CMP178 and CMP213 with the amino acid sequences of 27 known P genotypes[a]

Strain (origin)	P genotype	% Amino acid identity[b]			
		VP4		VP8*	
		CMP178	CMP213	CMP178	CMP213
RF (bovine)	P[1]	76.9	77.1	59.8	59.3
SA11 (simian)	P[2]	78.1	78.2	60.5	60.9
RRV (simian)	P[3]	77.3	77.3	59.7	59.7
RV-5 (human)	P[4]	68.8	68.8	51.4	51.4
UK (bovine)	P[5]	70.5	71.0	53.9	55.1
Gottfried (porcine)	P[6]	71.5	71.8	54.3	54.7
OSU (porcine)	P[7]	77.7	78.0	62.6	63.0
Wa (human)	P[8]	69.1	69.1	51.8	51.8
K8 (human)	P[9]	65.9	66.0	49.8	49.3
69M (human)	P[10]	76.3	76.7	57.2	57.6
B223 (bovine)	P[11]	58.2	58.2	35.1	35.1
H-2 (equine)	P[12]	74.8	74.8	58.0	57.2
MDR-13 (porcine)	P[13]	87.5	87.9	79.2	79.2
JP35-7 (porcine)	P[13] or P[22]?	—[c]	—	81.9	83.2
JP13-3 (porcine)	P[13] or P[22]?	—	—	81.9	83.2
ICB2212 (porcine)	P[13]?	—	—	83.2	82.3
ICB2219 (porcine)	P[13]?	—	—	82.3	81.4
A46 (porcine)	P[13]	89.3	89.7	83.7	83.2
HP113 (porcine)	P[13]	**92.2**	**92.2**	**88.1**	**87.2**
HP140 (porcine)	P[13]	**92.4**	**92.4**	**88.1**	**87.2**
PA169 (human)	P[14]	68.1	68.3	51.8	52.2
Lp14 (ovine)	P[15]	76.7	76.9	59.3	59.7
EB (murine)	P[16]	72.4	72.7	52.6	52.2
993-83 (bovine)	P[17]	59.9	59.9	60.0	60.0
L338 (equine)	P[18]	74.6	75.0	56.4	56.8
4F (porcine)	P[19]	71.8	71.8	52.6	52.6
EHP (murine)	P[20]	74.1	74.5	57.2	57.6
Hg18 (bovine)	P[21]	75.1	75.8	55.4	58.0
160/01 (lapine)	P[22]	—	—	80.6	80.6
229/01 (lapine)	P[22]	—	—	79.7	79.7
308/01 (lapine)	P[22]	—	—	77.9	78.4
3489/3 (lapine)	P[22]	—	—	81.0	81.0
A34 (porcine)	P[23]	—	—	61.8	62.2
TUCH (rhesus macaque)	P[24]	77.6	77.7	61.8	61.8
Dhaka6 (human)	P[25]	66.1	66.0	51.4	51.0
134/04-15 (porcine)	P[26]	84.7	84.8	69.2	69.2
CMP034 (porcine)	P[27]	71.0	71.0	57.1	56.0

[a] The GenBank accession numbers of VP4 genes are as indicated for the following strains: RF, U65924; SA11, M23188; RRV, M18736; RV-5, M32559; UK, M22306; Gottfried, M33516; OSU, X13190; Wa, M96825; K8, D90260; 69M, M60600; B223, D13394; H-2, L04638; MDR-13, L07886; PA169, D14724; Lp14, L11599; EB, U08419; 993-83, D16352; L338, D13399; 4F, L10359; EHP, U08424; Hg18, AF237665; 160/01, AF526374; A34, AY174094; TUCH, AY596189; Dhaka6, AY773004; 134/04-15, DQ061053; and CMP034, DQ534016.

[b] Boldface data indicate percentages of the highest sequence identity that CMP178 and CMP213 shared with the corresponding reference genotypes.

[c] —, no full-length VP4 sequence is available in the GenBank database.

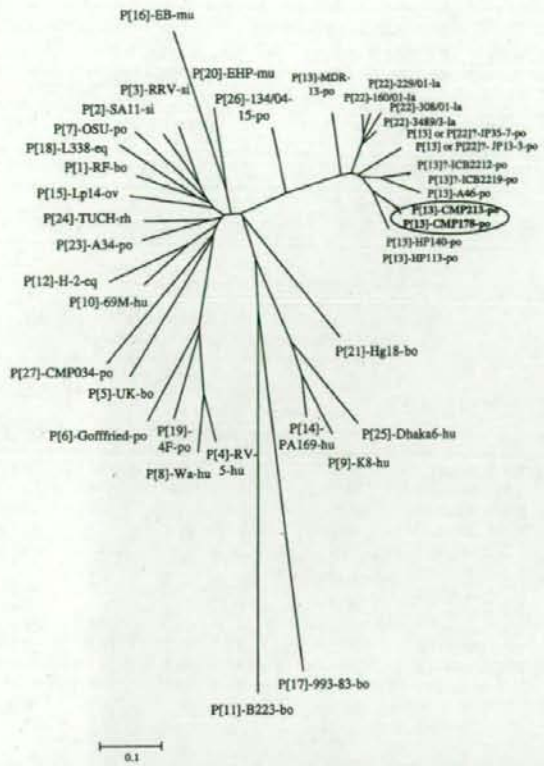

FIG. 2. Phylogenetic tree of the partial VP4 amino acid sequences displaying the relationships between PoRV strains CMP178, CMP213, and selected strains of the 27 P genotypes recognized to date. The following abbreviations are used to identify the species of strain origin: hu, human; eq, equine; po, porcine; bo, bovine; av, avian; pi, pigeon; mu, murine; si, simian; ov, ovine; la, lapine.

other reference strains of non-P[13] rotavirus (35.1% to 81.0% for both CMP178 and CMP213). Phylogenetic analysis supported the amino acid sequence alignments by showing that strains CMP178 and CMP213 clustered in the same branch with strains HP113 and HP140. Of note, although strains CMP178 and CMP213 were closely related to PoRV strains HP113 and HP140, they were rather distantly related to other P[13] PoRV strains and formed a distinct lineage (Fig. 2).

Taken together, the eight strains of P[13] PoRV described in this study comprised six strains of G3P[13] genotype and one strain each of the G4P[13] genotype and the G5P[13] genotype.

DISCUSSION

The eight strains of PoRV described in the present study were isolated from diarrheic piglets on several farms in Chiang Mai, Thailand, during epidemiological surveillance in 2002 and 2003. The initial characterization of the G and P genotypes of these strains by PCR by the use of multiple specific primer sets reported previously (6, 9, 24, 31, 40) revealed that six were G3, one was G4, and the other one was G nontypeable, while all were P nontypeable, as determined by PCR-based genotyping. We therefore further characterized those nontypeable strains by sequencing their VP7 and partial VP4 (VP8*) genes. The amino acid sequence of the VP8* fragment of these strains showed high degrees of identity, ranging from 94.7% to 100%, suggesting that they all belong to the same P genotype. In contrast, when the VP8* amino acid sequences of these strains were compared with those of the existing 27 P genotypes, only a low level of identity (35.1% to 88.1%) was observed (Table 2). In order to verify whether these strains belong to a novel P genotype or a variant strain of an existing known P genotype, the entire VP4 amino acid sequences were analyzed. Comparison of the full-length VP4 amino acid sequences of two representative strains, CMP178 and CMP213, with those of previously reported 27 P genotypes revealed sequence identities that ranged from 58.2% to 92.4% (Table 2). The high levels of amino acid identity were shared with two strains of PoRV recently isolated in India (7), strains HP113 and HP140, at 92.2% and 92.4%, respectively. On the basis of full-length VP4 amino acid sequence analysis, our strains most likely belong to the P[13] genotype. Phylogenetic analysis of the full-length amino acid sequences of the VP4 genes of strains CMP178 and CMP213 supported the sequence alignment data. CMP178 and CMP213 clustered tightly together with strains HP113 and HP140 in a single branch separated from other P[13] PoRV strains (Fig. 2).

Although strain CMP178 was initially identified as a G- and P-nontypeable strain by PCR-based genotyping, it was identified as a P[13] genotype strain (Table 2) that associated with the G5 genotype (Table 1) as a G5P[13] strain by amino acid sequence analyses of the VP4 and VP7 genes. Alignment of the G5-specific primer (SG 5) sequence (40) with the VP7 nucleotide sequence of CMP178 revealed four point mutations in the primer binding region (nt 180 to 200) at positions 183 (A to T), 186 (G to A), 187 (C to A), and 196 (G to A) (data not shown). These point mutations may lead to the failure of the binding of primer SG 5 at the target sequence in the VP4 gene of strain CMP178. This may explain why CMP178 was initially identified as G nontypeable by PCR-based genotyping. Additionally, CMP178 was also initially identified by PCR as P nontypeable, even though it was later identified as being of the P[13] genotype by VP4 sequence analysis, because no primer specific for P[13] has previously been reported in the literature.

Strain CMP213 was initially identified by PCR-based genotyping, and it was confirmed by VP7 sequence analysis (Table 1) to be genotype G3 with a P-nontypeable genotype and was later identified by VP4 sequence analysis to have the P[13] genotype (Table 2). On the basis of these data, CMP213 has a G3 genotype that exists in association with the P[13] genotype. In addition, among the P[13] strains of PoRV isolated in this study, one was found to have P[13] in combination with a G4 genotype (strain CMP077).

Altogether, the strains of PoRV isolated in the present study were P[13] in combination with several G types, including G3, G4, and G5. This finding implies multiple reassortment events and shows the diversity of the P[13] PoRV strains circulating in the pig population in Chiang Mai, Thailand.